Magnetic relaxation in dysprosium-dysprosium collisions

Bonna K. Newman,[1,3] Nathan Brahms,[2,3] Yat Shan Au,[2,3] Cort Johnson,[1,3] Colin B. Connolly,[2,3] John M. Doyle,[2,3] Daniel Kleppner,[1,3] and Thomas J. Greytak[1,3]

[1]*Massachusetts Institute of Technology*
[2]*Harvard University*
[3]*Harvard / MIT Center for Ultracold Atoms*

(Dated: December 2, 2010)

The collisional magnetic reorientation rate constant (g_R) is measured for magnetically trapped atomic dysprosium (Dy), an atom with large magnetic dipole moments. Using buffer gas cooling with cold helium, large numbers ($> 10^{11}$) of Dy are loaded into a magnetic trap and the buffer gas is subsequently removed. The decay of the trapped sample is governed by collisional reorientation of the atomic magnetic moments. We find $g_R = 1.9 \pm 0.5 \times 10^{-11}$ cm^3 s^{-1} at 390 mK. We also measure the magnetic reorientation rate constant of holmium (Ho), another highly magnetic atom, and find $g_R = 5 \pm 2 \times 10^{-12}$ cm^3 s^{-1} at 690 mK. The spin relaxation rates of these atoms are greater than expected for the magnetic dipole-dipole interaction, suggesting that another mechanism, such as an anisotropic electrostatic interaction, is responsible. Comparison with estimated elastic collision rates suggests that Dy and is a poor candidate for evaporative cooling in a magnetic trap.

PACS numbers: 34.20.Cf, 37.10.De

I. INTRODUCTION

The rare-earth atoms, dysprosium and holmium, have some of the largest atomic magnetic dipole moments, with $\mu_{\rm Dy} = 9.94\ \mu_B$ and $\mu_{\rm Ho} = 8.96$ [1]. Because the dipole-dipole interaction scales with the square of the dipole moment μ, there is much interest in creating ultracold degenerate gases of these atoms. Strong magnetic dipole interactions yield an array of new effects in degenerate gases, including new phase transitions [2], modifications of the BEC excitation spectrum [3], and trap-dependent BEC stability [4, 5]. The study of magnetic dipole interactions in cold gases can also serve as a model for the behavior of the electric dipole interaction of trapped polar molecules; a new and increasingly promising area of ultracold degenerate systems. Further, the electronic spectrum of Dy offers opportunities for precision measurements [6–9], quantum computation [10], and a test of parity nonconservation [11].

The complex electronic structures of Dy and Ho that lead to the large magnetic moments also makes them more difficult to trap and cool than closed shell or S-state atoms, which are the most commonly studied degenerate gases. The isotropic electrostatic structure of closed-shell atoms assures that spherically symmetric interactions dominate collision processes. For atoms whose outermost electronic shell has non-zero orbital angular momentum, or open-shell atoms, the electrostatic anisotropic interaction can play the determining role in trap loss and limit the efficiency of evaporative cooling. For instance, experiments with metastable Sr [12, 13] and Yb [14], and theory with O [15] show that these atoms undergo magnetic moment reorientation in nearly every collision due to electron anisotropy. Consequently, collision processes in cold gases with anisotropic electrostatic interactions present a new challenge to theory and a new area of exploration for experiment [16]. Both Dy and Ho have an unfilled, highly anisotropic $4f_{10}$ shell.

Recent experiments in trapping large numbers of Dy atoms using ^{3}He buffer gas cooling [17] have demonstrated that in collisions with He, Dy exhibits suppressed anisotropy, leading to a large ($> 10^5$) ratio of elastic to inelastic collisions and allowing for efficient cooling with a He buffer gas. Theory suggests [18, 19] that this suppression is due to the filled 5s and 6s shells which extend to a larger radius than the more tightly bound unfilled 4f shell. The interplay of the short-range anisotropic electrostatic interaction and the magnetic dipole-dipole interaction may offer novel ultracold collisional physics. The study of these interactions in the sub-Kelvin regime is important for cooling of a broader range of atoms to ultracold temperatures.

Using buffer gas cooling with ^{3}He we have magnetically trapped large numbers ($> 10^{11}$) of Dy atoms at temperatures around 400 mK and measured the rate of magnetic relaxation in collisions between two Dy atoms. After removing the buffer gas, we monitor the trap population by measuring the optical density using atomic absorption spectroscopy. From this evolution we measure the rate of trap decay due to inelastic two-body collisions and extrapolate the magnetic reorientation rate constant. We perform a similar measurement in at trap of Ho atoms at 700 mK. We observe inelastic spin reorientation rates that are at least an order of magnitude larger than expected due to the magnetic dipole-dipole interaction. Comparison of these rates to other buffer-gas cooled atoms [20–22] suggest that anisotropic electrostatic interactions dominate the inelastic collision cross-section for these open-shell atoms.

II. EXPERIMENTAL METHODS

The measurements were conducted in a buffer gas cooling apparatus. The essentials of the experimental apparatus are depicted in Fig. 1 and described in more detail elsewhere [23]. The apparatus consists of a G10 Garolite composite cell within the bore of a superconducting anti-Helmholtz magnet. The magnet forms a linear quadrupole trap with the trapping volume defined by the magnetic field at the cell walls, which can be as large as 4 T. Majorana trap losses are negligible in our experiment at the temperatures and trap depths used. The cell is thermally anchored via a flexible copper heat link to the cold plate of a dilution refrigerator at 30 mK. A heater is used to control the cell temperature between 100 mK and 1 K. Copper wires running the length of the cell provide thermal contact between the cell top and bottom. The lower chamber of the cell forms the trapping chamber, into which ^{3}He is introduced via a fill line. The upper chamber holds a charcoal sorbtion pump. The two chambers are separated by a cryogenic, nonmagnetic valve that is opened in 40 ms via an external cable.

A probe laser of diameter 5 ± 1 mm is tuned to resonance with the trapped ground state atoms. It passes through the center of the atom cloud via a sapphire window at the cell bottom. The laser is retroreflected from a mirror suspended at the top of the trapping chamber. The reflected light beam, which has passed through the trapped atoms twice, is compared to a reference beam, resulting in a measurement of atomic optical density. The probe beam power is far below the saturation of the transition (1 μW) and is shuttered unless the trap population is being measured in order to minimize its influence on trap lifetime. The probe laser is scanned across the Dy $^5I_8 \rightarrow {}^5(8,1)_7$ transition at 404.71 nm. (The numbers in parentheses indicate the angular quantum numbers of the excited state in the J–J coupling scheme.) We interrogate the Ho $^4H_{15/2} \rightarrow {}^4(15/2,1)_{17/2}$ transition at 410.5 nm. [1]. Optical density of the atom cloud is measured at each point in the spectrum.

Initially, the trapping region is filled with ^{3}He atoms at a density of $\sim 10^{16}$ cm^{-3} and a temperature chosen between 250 mK and 600 mK. With the trap on, Dy is ablated using a 10 ns pulse from a 532 nm Nd:YAG laser. The gas of hot atoms liberated by the ablation pulse is translationally thermalized to the buffer gas temperature after $\sim$ 100 elastic collisions with the buffer gas. After waiting 200 ms for the atoms to diffuse into the center of the magnetic trap, the buffer gas is removed by opening the cryogenic valve, reducing the ^{3}He density to $< 10^{10}$ cm^{-3} in $\sim$ 100 ms. The majority of the atoms ($> 80\%$) remain trapped. At this point, the atom population is measured as a function of time to determine the atomic inelastic collision rate.

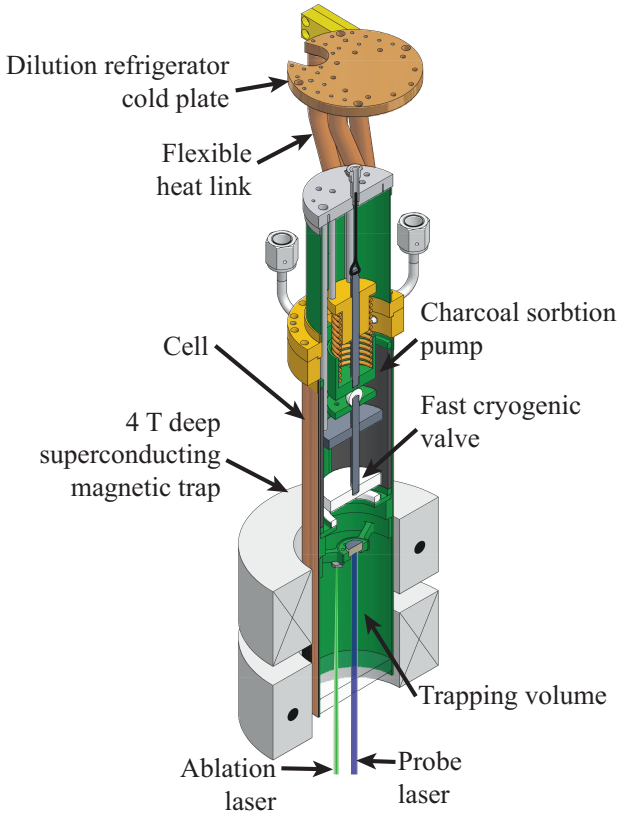

FIG. 1. The experimental cell

III. RESULTS

We extract physical parameters of the atom cloud, such as atom number, temperature, and state distribution, by fitting the observed atomic optical density spectrum to a simulation [21, 27] of the optical absorption of the trapped atoms. To accurately simulate the spectrum, we specify all the related spectroscopic parameters for the transition: the isotopic distribution and frequency shifts, Landé g-factors, and ground and excited state quantum numbers and hyperfine constants. The parameters used are summarized in Table I. Most of these constants are found in the literature [1, 26]. However, the Dy $^5(8,1)_7$ state isotope shifts and hyperfine constants could not be located. Instead, these constants were approximated by fitting the relative heights and locations of the common isotope peaks in a Dy spectrum taken at zero magnetic field; see Fig. 2.

At low He densities, the evolution of the number N_a of atoms in the $m_J = J$ stretched state can be described by [28]

$$\dot{N}_a = -g_b n_b N_a - (f_a g_a + g_R)\, N_a^2/8V, \qquad (1)$$

where n_b is the residual density of ^{3}He in the cell, and $g_b n_b$ is the loss rate due to atom–^{3}He collisions. g_a is the

Atom	Term[a]	Landé g_J[a] Ground	Excited	Iso.	Abund.[a]	I[a]	Shift[b] (MHz)	Ground hyperfine[c] A (MHz)	B (MHz)	Excited hyperfine[d] A (MHz)	B (MHz)
Dy	$^5I_8 \rightarrow {}^5(8,1)_7$	1.24	1.26	164	0.282	0	0				
				163	0.249	5/2	130	162	1152	190 ± 10	1000 ± 200
				162	0.255	0	370				
				161	0.189	5/2	510	-116	1091	-140 ± 10	1700 ± 200
				160	0.0234	0	810				
Ho	$^4H_{15/2} \rightarrow$ $^4(15/2,1)_{17/2}$	1.20	1.18	165	1.0	7/2		800.583	-1688	653 ± 2	-500 ± 200

[a] From [1], except the excited g_J, which is calculated from the J–J coupling quantum numbers.
[b] Estimated from 0-field fit.
[c] From [24, 25].
[d] Dy values estimated from 0-field fit, Ho values from [26].

TABLE I. Spectroscopic parameters used in this work. For parameters not available in the literature, we estimate the values by fitting the isotope peak heights and locations in spectra taken at zero magnetic field.

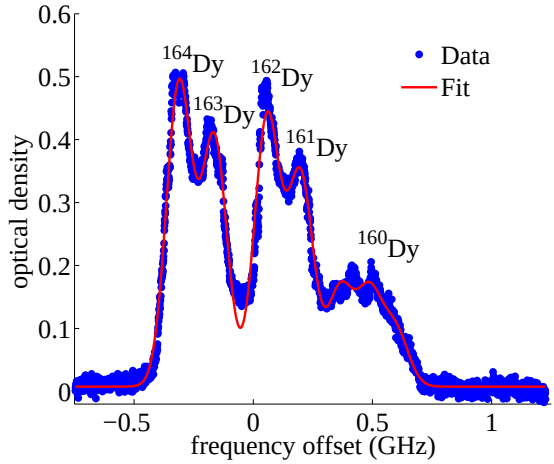

FIG. 2. Dy spectrum at zero magnetic field. There are five isotopes of Dy with occupation greater than 2%. From the spacings of the isotope peaks for ^{165}Dy, ^{163}Dy, and ^{161}Dy at zero field, we estimate the hyperfine constants (A, B) for the $^5(8,1)_7$ excited state (see Table I).

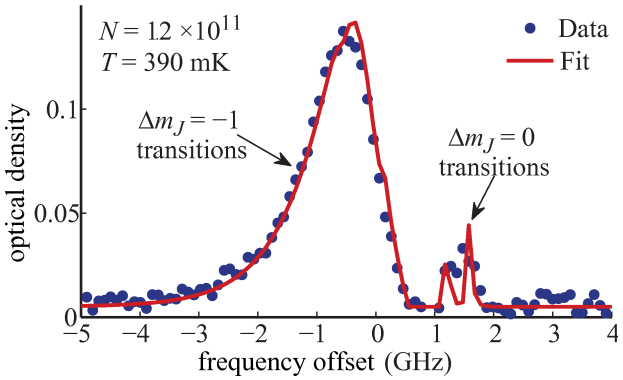

FIG. 3. Measured spectrum of Dy in a 1.9 T deep magnetic trap, 2 s after ablation. The line shows a fit to the spectrum, yielding $N = 1.2 \times 10^{11}$ and $T = 390$ mK. By comparing the optical density of the $\Delta m_J = -1$ peak to that of the $\Delta m_J = 0$ peak, we measure a stretched $m_J = 8$ population of 80%.

rate coefficient for elastic atom–atom collisions, and g_R is the rate coefficient for magnetic moment reorienting atom–atom collisions. V is the effective volume of the trap; the factor of 1/8 in Eqn. (1) arises from averaging the square of the local atom density over the linear quadrupole trap. f_a is the constant of proportionality between the rate of elastic atom–atom collisions and the rate of evaporation over the trap edge. For atoms at temperature T_a and trap depth $U_{\rm trap}$, $f_a \sim e^{-U_{\rm trap}/k_B T_a}$.

If the first term in Eqn. (1) dominates, the trap population decays exponentially and is referred to as "one-body" loss; the rate is proportional to N_a. However, if the second term dominates, the atom number decay obeys the "two-body" equation

$$N_a(t) = \frac{N_0}{N_0 g t/8V + 1}, \tag{2}$$

with

$$g = f_a(U_{\rm trap}, T_a)\, g_a + g_R. \tag{3}$$

For this measurement, we performed experiments at different values of $U_{\rm trap}$ but constant T_a in order to test the first term of Eqn. (3). We find that g does not vary systematically as a function of $U_{\rm trap}$, suggesting that f_a is small in our trap and losses due to evaporation over the trap edge are negligible. Therefore, in the following analysis we assume $g = g_R$.

Fig. 3 shows a typical spectrum of trapped Dy two seconds after buffer gas removal. The spectral fit yields $N = 1.2 \times 10^{11}$ and T =390 mK in a 1.9 T deep trap. This corresponds to a ratio of $U_{\rm trap}$ to $k_B T_a$ of 12.5 and an

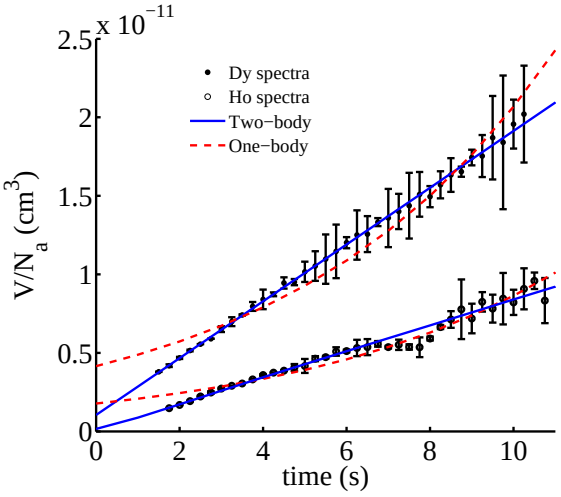

FIG. 4. Reciprocal of atom number density evolution of trapped Dy atoms. Each point is the result of fitting temperature and atom number of the atomic spectrum at each time (e.g. Fig. 3. Temperature is 390 ± 30 mK and 690 ± 50mK for Dy and Ho respectively, for the lifetime of the trap. Plotted as V/N_a versus time, linear "two-body" decay is easily distinguished from exponential "one-body" decay. g_R is derived from the slope of the two-body fit.

atom cloud approximately 6 mm in diameter, exploring an average field of 0.2 T. Atoms with $m_J \leq 3$ will not be trapped. Atoms with $m_J > 4$ remain weakly trapped and will contribute to the spectra. However, we observe a $J \rightarrow J-1$ transition. Therefore, the Dy stretched state $m_J = 8$ population can only undergo $\Delta m_J = -1$ optical transitions. Trapped atoms in lower m_J levels contribute to the $\Delta m_J = 0$ transition signal. This allows us to estimate the fraction of Dy atoms in the stretched state by comparing the optical absorption in $\Delta m_J = -1$ transitions to that in $\Delta m_J = 0$ transitions. We find that after two seconds more than 80% of the Dy are in the $m_J = 8$ state and the atoms remain similarly distributed for the lifetime of the trap. This suggests that a fast mechanism, such as spin exchange, is working to purify the population of the trap into the stretched state.

Spin exchange is forbidden in stretched state atom collisions [29]. Two-body decay of this population therefore results from inelastic processes which couple the magnetic moment to a non-spin angular degree of freedom (e.g. collisional or electronic angular momentum). Because our trapped population is mostly stretched state atoms, we assign the measured atom loss to inelastic magnetic moment reorienting collisions. Thermal excitations of atoms in non-stretched states introduce a small systematic error ($< +10\%$) in our inelastic rate measurement.

To confirm that the decay is due to a two-body process, we plot the inverse of the Dy atom number as a function of time in Fig. 4. In this plot, two-body decay appears as a straight line with slope $g_R/8$ while one-body decay would appear as a positive exponential. We fit to a one-body, two-body, and combined decay profiles. We find that a two-body fit with no one-body component results in the smallest reduced χ^2. This confirms that the He buffer gas has been successfully removed and we are measuring losses due only to ground state atom-atom interactions. We measure the rate of lifetime-limiting inelastic Dy–Dy collisions to be $g_R = 1.9 \pm 0.5 \times 10^{-11}$ cm^3 s^{-1} at 390 ± 30 mK. This corresponds to an inelastic cross section of 1.9×10^{-14} cm^2.

We also measured the rate of two-body trap loss of cold atomic holmium–holmium collisions in our apparatus; the evolution of the Ho trap population is also shown in Fig. 4. We derive the collision rate using the spectroscopic parameters in Table I and the same procedure as described for Dy. We find that the magnetic reorientation rate for Ho is $g_R = 5 \pm 2 \times 10^{-12}$ cm^3 s^{-1} at 690 ± 50 mK. We find the Ho decay is best fit by the two-body decay model, indicating successful removal of the buffer gas. However, the error on this measurement is larger than in the Dy experiment due to smaller numbers of trapped atoms and the overlap of spectral features of the hyperfine states. Uncertainty of the state distribution makes it difficult to quantify the effect of thermal excitations on this system; the actual Ho–Ho inelastic collision rate could be twice as large as the loss rate we measure [30].

IV. DISCUSSION

Elastic Collisions. In order to achieve efficient evaporative cooling, it is necessary to have multiple elastic collisions for every inelastic collision that leads to trap loss. A reasonable estimate for the Dy–Dy elastic collision cross-section at sub-Kelvin temperatures can be obtained by taking half of the unitarity limit [31]:

$$\sigma_{\rm el} \approx \frac{\hbar^2 \pi}{mE} \sum_{\ell} (2\ell + 1). \qquad (4)$$

At 390 mK, we can expect multiple partial waves (ℓ up to 30) to contribute to elastic scattering and $\sigma_{\rm el} \approx 4.5 \times 10^{-13}$ cm^2, with larger values possible if shape resonances are present. This estimate implies that Dy should undergo only twenty thermalizing elastic collisions for every inelastic loss, making evaporative cooling rather inefficient. This conclusion is supported by the prohibitively large loss of trapped atoms observed when we attempt to evaporatively cool the sample.

Inelastic Collisions. Different physical mechanisms are responsible for two-body inelastic collision processes between open shell magnetically trapped atoms in the stretched state; the magnetic dipole interaction and electrostatic interactions of the valence shells may be expected to play a significant role in this system. The following discussion will show that the magnetic dipole interaction, though very strong between highly magnetic atoms, does not explain the rapid collisional reorientation rate we measure.

The magnetic dipole interaction has been well studied in alkali metal gases. The Hamiltonian for a collision of two dipolar atoms can be written as

$$H(\vec{r}) = \frac{\mu_0 \mu_B^2 g_J^2}{4\pi r^3}[\vec{\mathbf{J}}_1 \cdot \vec{\mathbf{J}}_2 - 3(\vec{\mathbf{J}}_1 \cdot \hat{r})(\vec{\mathbf{J}}_2 \cdot \hat{r})] + V(\vec{r}) \quad (5)$$

where μ_0 is the magnetic constant, $\vec{r}$ is the vector of internuclear separation, and all other interatomic interactions are included in $V(\vec{r})$.

Using the Born approximation, the dipolar relaxation rate of spin polarized atoms due to dipolar interactions can be shown to scale according to [32]:

$$g_{\rm dip} \propto J^3 g_J^4 \quad (6)$$

where J is the total angular momentum quantum number, and g_J is the Landé g-factor. While the actual cross-section depends on the exact form of $V(\vec{r})$, an estimate of the dipolar relaxation rate is made by scaling measurements from other atomic systems using Eqn. (6). We estimate expected Dy relaxation rates from measurements of inelastic rates for atoms whose reorientation is dominated by magnetic dipolar relaxation. Using data from trapped Cr at 200 mK [20] and Eu at 160 mK [21] we compare our measured rate constant of $g_R = 1.9 \pm 0.5 \times 10^{-11}$ cm^3 s^{-1} to the expected $g_{\rm Dy} = 3.2 \times 10^{-13}$ cm^3 s^{-1} and 1.1×10^{-12} cm^3 s^{-1} scaled for temperature and magnetic moment from Eu and Cr respectively. Our measured spin relaxation rate is one to two orders of magnitude larger than these estimated magnetic dipolar relaxation rates, suggesting that dipolar relaxation is not solely responsible for this fast decay.

We also find that the rates for Ho and Dy are significantly smaller than rates in similarly trapped Er and Tm, 3.0 and 1.1×10^{-10} cm^3 s^{-1}, respectively [22], which have smaller magnetic dipoles. This observation further suggests that magnetic dipole-dipole interactions are not the dominate mechanism for spin relaxation in collisions between rare-earth atoms. The interaction of anisotropic electrostatic potentials could be responsible for the large rate of spin relaxation and short trap lifetime. However, theory is needed to confirm this.

Recently, a magneto-optical trap of 5×10^8 Dy atoms at temperatures around 500 μK was reported in the literature [33]. The inelastic two-body loss rate of ^{164}Dy was measured to be 2.1×10^{-10} cm^3 s^{-1}. Comparison with our measurement at higher temperatures suggests a temperature dependence of the total inelastic scattering cross section as $E \to 0$ [34]. Further experiments will be necessary to fully understand these collisional processes in complex atoms.

V. CONCLUSION

Our determination of the inelastic cross section and estimate of the elastic cross-section indicates that evaporative cooling of Dy in a magnetic trap will be very inefficient. Despite this limitation, we were able to adiabatically cool $> 10^9$ Dy atoms to 50 mK in our buffer gas apparatus by rapidly changing the magnetic gradient. If cooling to a few mK can be accomplished, it may be possible to load a far off-resonant dipole trap (FORT) [35] using additional laser cooling. However, care must be taken to deal with scattering into dark states. A 5 mK deep dipole trap for Dy could be constructed using 200 mW of 420 nm light (available from a doubled Ti:Al_2O_3 laser), detuned two THz from the $\Delta J = 1$ transition and focused to a 30 μm waist, having an absorption rate of 400 s^{-1}. Once in an optical trap, efficient cooling could be achieved using evaporative or demagnetization cooling [36].

Dy is a promising atom for studying the effects and role of large magnetic dipole interactions. However, we find that the large inelastic collision rate, possibly due to anisotropic electrostatic interactions, is prohibitive to using evaporative cooling techniques of magnetically trapped atoms in the low-field-seeking state. Other trapping and cooling schemes will be necessary to reach the degenerate regime.

The authors acknowledge financial support from the National Science Foundation (Grant No. PHY-0757157).

[1] C. E. Moore, *Atomic Energy Levels As Derived From the Analyses of Optical Spectra*, 35th ed., NSRDS-NBS, Vol. 2 (National Bureau of Standards, 1971).
[2] K. Góral, L. Santos, and M. Lewenstein, Phys. Rev. Lett., **88**, 170406 (2002).
[3] L. Santos, G. V. Shlyapnikov, P. Zoller, and M. Lewenstein, Phys. Rev. Lett., **85**, 1791 (2000).
[4] T. Koch, T. Lahaye, J. Metz, B. Frhlich, A. Griesmaier, and T. Pfau, Nature Phys., **4**, 218 (2008).
[5] S. Yi and L. You, Phys. Rev. A, **63**, 053607 (2001).
[6] A. T. Nguyen, D. Budker, S. K. Lamoreaux, and J. R. Torgerson, Phys. Rev. A, **69**, 022105 (2004).
[7] A. Cingoz, A. Lapierre, A.-T. Nguyen, N. Leefer, D. Budker, S. K. Lamoreaux, and J. R. Torgerson, Physical Review Letters, **98**, 040801 (2007).
[8] V. A. Dzuba and V. V. Flambaum, Physical Review A (Atomic, Molecular, and Optical Physics), **72**, 052514 (2005).
[9] V. A. Dzuba and V. V. Flambaum, Physical Review A (Atomic, Molecular, and Optical Physics), **77**, 012515 (2008).
[10] D. DeMille, Phys. Rev. Lett., **88**, 067901 (2002).
[11] D. Budker, D. DeMille, E. D. Commins, and M. S. Zolotorev, Phys. Rev. Lett., **70**, 3019 (1993).
[12] V. Kokoouline, R. Santra, and C. H. Greene, Phys. Rev. Lett., **90**, 253201 (2003).
[13] S. B. Nagel, C. E. Simien, S. Laha, P. Gupta, V. S. Ashoka, and T. C. Killian, Phys. Rev. A, **67**, 011401

(2003).
[14] A. Yamaguchi, S. Uetake, D. Hashimoto, J. M. Doyle, and Y. Takahashi, Physical Review Letters, **101**, 233002 (2008).
[15] R. V. Krems and A. Dalgarno, Phys. Rev. A, **68**, 013406 (2003).
[16] R. Krems, G. Groenenboom, and A. Dalgarno, Journal of Physical Chemistry A, **108**, 8941 (2004), ISSN 1089-5639.
[17] C. I. Hancox, S. C. Doret, M. Hummon, L. T.Luo, and J. M. Doyle, Nature, **431**, 281 (2004).
[18] R. Krems and A. Buchachenko, Journal of Chemical Physics, **123**, 101101 (2005).
[19] R. V. Krems, J. Kłos, M. F. Rode, M. M. Szcześniak, G. Chałasiński, and A. Dalgarno, Physical Review Letters, **94**, 013202 (2005).
[20] J. D. Weinstein, R. deCarvalho, C. I. Hancox, and J. M. Doyle, Phys. Rev. A, **65**, 021604 (2002).
[21] J. Kim, B. Friedrich, D. P. Katz, D. Patterson, J. D. Weinstein, R. DeCarvalho, and J. M. Doyle, Phys. Rev. Lett., **78**, 3665 (1997).
[22] C. B. Connolly, Y. S. Au, S. C. Doret, W. Ketterle, and J. M. Doyle, Phys. Rev. A, **81**, 010702 (2010).
[23] N. Brahms, B. Newman, C. Johnson, T. Greytak, D. Kleppner, and J. Doyle, Physics Review Letters, **101**, 103002 (2008).
[24] J. Ferch, W. Dankwort, and H. Gebauer, Physics Letters, **49A**, 287288 (1974).
[25] W. Dankwort, J. Ferch, and H. Gebauer, Zeitschrift fur Physik, **267**, 229 (1974).
[26] C. Hancox, *Magnetic Trapping of transition-metals and rare-earth atoms using buffer-gas loading*, Ph.D. thesis, Harvard University (2005).
[27] N. C. Brahms, *Trapping of 1 μ_B atoms using buffer gas loading*, Ph.D. thesis, Harvard University (2008).
[28] B. Newman, *Trapped atom collisions and evaporative cooling of non-S state atoms*, Ph.D. thesis, MIT (2008).
[29] W. Ketterle and N. J. V. Druten, Advances in Atomic, Molecular, and Optical Physics, **37**, 181 (1996).
[30] C. Johnson, B. Newman, N. Brahms, J. M. Doyle, D. Kleppner, and T. J. Greytak, Phys. Rev. A (2010).
[31] E. Merzbacher, *Quantum Mechanics*, 2nd ed. (Wiley, 1970).
[32] J. Stuhler, A. Griesmaier, T. Koch, M. Fattori, T. Pfau, S. Giovanazzi, P. Pedri, and L. Santos, Physical Review Letters, **95**, 150406 (2005).
[33] M. Lu, S. H. Youn, and B. L. Lev, Phys. Rev. Lett., **104**, 063001 (2010).
[34] J. Weiner, V. S. Bagnato, S. Zilio, and P. S. Julienne, Rev. Mod. Phys., **71**, 1 (1999).
[35] H. J. Metcalf and P. van der Straten, *Laser cooling and trapping*, 1st ed. (Springer, 1999).
[36] M. Fattori, T. Koch, S. Goetz, A. Griesmaier, J. S. S. Hensler, and T. Pfau, Nature Phys., **2**, 765 (2006).